Check for updates

Purification and rapid dissolution of potassium sulfate in aqueous solutions

Shoujiang Li,[a] Kaige Sun,[a] Yunliang Zhao, [ID] *[ab] Guihua Nie[a] and Shaoxian Song[b]

Water soluble potassium sulfate dissolves rapidly and completely in water. Its main characteristics are purity and dissolution rate. In this study, the purification and rapid dissolution of potassium salt (K_2SO_4) separated from potassium brine deposits collected from Lop Nur basin of China (referred to as LN K_2SO_4) were studied for utilization in agricultural farming as a potash fertilizer. First, the dissolving-crystallizing process was conducted to remove the insoluble content and improve the purity of K_2SO_4. Second, physical modification of K_2SO_4 surfaces was accomplished based on the Noyes–Whitney equation. The results showed that the water insoluble content could be completely removed and the purity of K_2SO_4 reached 100% in the purification process. The dissolution rate was significantly improved with the help of environmentally-friendly additives such as sodium tripolyphosphate (STPP)/urea phosphate (UP). These additives ameliorated the diffusion coefficient (D) and the diffusion layer thickness (h) for K_2SO_4. Results also demonstrated that a larger K_2SO_4 surface area (S) induced a higher dissolution rate.

1 Introduction

Potassium is one of the three essential elements for plants to maintain proper growth.[1–5] Potash fertilizers used in agriculture usually contain two types: one is potassium chloride (KCl), which is harmful to some crops, increases soil salinity and pH of the soil, and the other is potassium sulfate (K_2SO_4), which is a chlorine-free, high-quality, potent potash fertilizer, especially indispensable for tobacco, tea, potatoes, watermelon, sugar beets and other economic crops that are sensitive to chlorine.[6–9]

Fully water-soluble potassium sulfate can dissolve rapidly and completely in water, allowing it to be more efficiently absorbed and utilized by crops. More importantly, K_2SO_4 can be applied in agricultural facilities for processes such as sprinkler irrigation and drip irrigation. Overall, this allows for the integration of water and fertilizer, a reduction in water usage, fertilizer-saving, reduced labor and increased production.[10,11] As a result, water-soluble fertilizer is a promising candidate for the simultaneous application of water and fertilizer technology for reduced water consumption in agricultural applications.

Lop Nur salt lake, located in the eastern Tarim basin, contains the biggest potassium brine deposits discovered in China. These deposits also contain a magnesium sulfate subtype brine and can be used to produce potassium sulfate fertilizers.[12,13] Through the exploitation and utilization of Lop Nur salt lake, SDIC Xinjiang Lop Nur Potash Co. Ltd. (SLNP) has

become the biggest K_2SO_4 production company in the world with a K_2SO_4 yield of 1.6 million ton per year.[14,15] The insoluble content in K_2SO_4 production affects not only the purity of K_2SO_4, but also the dissolution rate. However, Lop Nur agricultural K_2SO_4 (LN K_2SO_4) contains about 1 wt% insoluble residue, which decreased the purity of K_2SO_4 and made it dissolve slowly and incompletely. Moreover, the purity of LN K_2SO_4 does not meet the national standard for water soluble fertilizer HG/T4365-2012, where the insoluble content must be less than 0.5 wt%. Therefore, it is necessary to investigate the purification of LN K_2SO_4.

The process for dissolving a solid requires two consecutive stages. In the first stage, solute molecules are released from the solid surface into the solution. In the second stage, dissolved molecules are transferred from the solid–liquid interface to the solution by diffusion or convection.[16–18] The dissolution process can be explained by the Noyes–Whitney[19,20] equation:[19,20]

$$\frac{dm}{dt} = VM\frac{dC}{dt} = \frac{MDS}{h}(C_s - C) \tag{1}$$

where dm/dt represents the dissolution rate, S is the surface area of the solid particle, D is the diffusion coefficient, C and C_s represent the concentrations of the solute in the solution at a certain time (t) and solubility, respectively, and M and h are the relative molecular mass and diffusion layer thickness of the solute, respectively. This equation means that the dissolution rate can be controlled by regulating parameters like D, S and h.

Potassium sulfate dissolution has drawn widespread attention. Kubota stated that traces of foreign ions (trivalent chromium and trivalent iron) have a significant effect on the

[a]School of Resources and Environmental Engineering, Wuhan University of Technology, Luoshi Road 122, Wuhan, Hubei, 430070, China. E-mail: zyl286@whut.edu.cn

[b]Hubei Key Laboratory of Mineral Resources Processing and Environment, Wuhan University of Technology, Luoshi Road 122, Wuhan, Hubei, 430070, China

dissolution rates of K_2SO_4 crystals.[21–23] Furthermore, the dissolution kinetics of K_2SO_4 crystals were studied with an ion selective electrode. The effects of hydrodynamics on the dissolution were also investigated.[24] However, the above research studies were based on a more ideal situation or pure K_2SO_4 crystal samples. No profound study has been performed on agricultural K_2SO_4 and its rapid dissolution. Thus in this paper, an attempt was made to study the purification and rapid dissolution behavior of potassium sulfate. First, Lop Nur agricultural K_2SO_4 (LN K_2SO_4) was used as a raw material to remove the insoluble content by a purification process. The Noyes–Whitney equation was then applied to analyze the K_2SO_4 dissolution mechanism. The physical properties of K_2SO_4 were modified with the help of surfactants. Accordingly, the rapid dissolving process was determined.

2 Experimental

2.1 Materials

Agricultural potassium sulfate (LN K_2SO_4) was obtained from SDIC Xinjiang Lop Nur Potash Co. Ltd., China. Chemical grade polyethylene glycol 1000 (PEG 1000), sodium tripolyphosphate (STPP), and analytical grade reagents for gravimetric methods and Volhard method (sodium tetraphenylborate, ethylenediaminetetraacetic acid disodium salt, ammonium iron sulfate, $BaCl_2$ and $AgNO_3$) were purchased from Sinopharm Chemical Reagent Co. Ltd. Industrial grade urea phosphate (UP) was purchased from Tianjin Kemiou Chemical Reagent Co. Ltd. Tap water was used in all experiments and its physicochemical properties are shown in Table 1. The concentration of metal ions (K^+, Na^+, Mg^{2+}, Ca^{2+}) was determined by an atomic absorption spectrophotometer (AAS, AA-6880 SHIMADZU, Japan). The concentration of SO_4^{2-} and Cl^- anions was determined by the barium chloride gravimetric method and the Volhard method, respectively.

2.2 Characterization

The chemical composition of LN K_2SO_4 and purified LN K_2SO_4 (PLN K_2SO_4) are shown in Tables 2 and 3, respectively. The potassium content (wt%) was determined by the potassium tetraphenylborate gravimetric method. The SO_4^{2-} and Cl^- contents were determined by the barium chloride gravimetric method and the Volhard method, respectively. The Na^+, Mg^{2+}, Ca^{2+} metal ion contents were determined by AAS.

The particle size was related to the surface area, which was significant for the dissolution rate according to the Noyes–Whitney equation. The size distribution of LN K_2SO_4 was obtained with wet sieves. The results are listed in Table 4. It can be seen that the size distribution of LN K_2SO_4 was $-150 + 105$ μm up to 60%.

2.3 Purification of Lop Nur agricultural potassium sulfate

The solubility of K_2SO_4 was positively correlated with temperature. Purification was achieved by dissolving agricultural potassium sulfate at a high temperature, filtering to remove the insoluble content, and then crystallizing at a low temperature. The purification experiment was carried out as follows. First, a certain mass of LN K_2SO_4 was added to a three-necked bottle that contained 1 L of water to obtain the desired liquid to solid ratio. The mixture was then stirred at a speed of 300 rpm for 10 min to achieve a dissolution equilibrium at the desired temperature (100 °C, 80 °C or 60 °C). Afterwards, the residues were separated at the above desired temperature using a qualitative filter paper. The filtrate was placed in an alternating damp heat apparatus for spontaneous crystallization at the desired temperature (0–30 °C). After a certain crystallization time, the

Table 1 Physicochemical properties of tap water

Physicochemical properties	K^+ (mg L^{-1})	Na^+ (mg L^{-1})	Mg^{2+} (mg L^{-1})	Ca^{2+} (mg L^{-1})	Cl^- (mg L^{-1})	SO_4^{2-} (mg L^{-1})	pH	Conductivity (μS cm^{-1})
	92.5	4.8	28.8	55.2	117	142	7.31	344.6

Table 2 Chemical analysis of LN K_2SO_4

| Sample | Weight (%) | | | | | | | |
	K_2O	SO_4^{2-}	Mg^{2+}	Cl^-	Ca^{2+}	Na^+	H_2O	Insolubles
LN K_2SO_4	49.91 ± 0.69	53.79 ± 1.21	0.213 ± 0.03	1.233 ± 0.27	0.16 ± 0.04	0.19 ± 0.07	0.21 ± 0.006	1.18 ± 0.37

Table 3 Chemical analysis of PLN K_2SO_4

| Sample | Weight (%) | | | | | | |
	K_2O	SO_4^{2-}	Mg^{2+}	Cl^-	Ca^{2+}	Na^+	Insolubles
PLN K_2SO_4	54.67 ± 0.97	54.52 ± 0.80	0.0037 ± 0.001	0.057 ± 0.002	0.0167 ± 0.006	0.017 ± 0.005	0

Table 4 Particle size distribution for LN K_2SO_4

LN K_2SO_4	Size fraction (μm)							
	+450	−450 + 300	−300 + 150	−150 + 105	−105 + 74	−74 + 45	−45	Total
Yield (%)	0.33	6.73	18.64	60.49	1.26	11.2	1.35	100

solid phase was separated from the solution using a qualitative filter paper. The obtained solid was dried at 105 °C in an oven until a constant weight was recorded. Finally, the purified LN K_2SO_4 (PLN K_2SO_4) was obtained. The chemical composition of PLN K_2SO_4 was determined using the same method as that for LN K_2SO_4. The crystallization yield was calculated by using the following equation:

$$y = \frac{m_1}{m_2} \times 100\% \qquad (2)$$

where m_1 and m_2 represent the mass of the crystallization solid and dosage of LN K_2SO_4.

2.4 Rapid dissolution of potassium sulfate

To improve the dissolution rate of K_2SO_4, the purified LN K_2SO_4 (PLN K_2SO_4) product was mixed with some additives such as dispersants, wetting agents and surfactants. The procedures were as follows: first, additives with a different mass ratio (accounting for the mass of PLN K_2SO_4), and PLN K_2SO_4 were mechanically ground to form a homogeneous mixture. The mixture was then crushed at different times with a high-speed crusher (FW-100, China) to achieve a suitable granular grade. Afterwards, 100 g of the above mixture was added to 1 L of water at room temperature under a stirring speed of 150 rpm. An electrical conductivity meter (A215, ORION, USA) was used to determine the end of the dissolution process. The conductivity of the solution increased as the dissolution process progressed and then reached equilibrium when the dissolution was completed. Meanwhile, the dissolution time was recorded when the conductivity reached equilibrium. The dissolution rate was expressed in terms of dissolution time.

3 Results and discussion

3.1 Purification of Lop Nur agricultural potassium sulfate

It can be seen from Table 2 that the water insoluble content in the LN K_2SO_4 samples was 0.76 wt%, which was higher than the national standard of 0.5 wt%. The high insoluble content had a negative effect on the dissolution of LN K_2SO_4. Purification significantly and efficiently solved the problem. After comparing Table 3 with Table 2, it can be obviously seen that the insoluble content was efficiently removed and that the impurity content for the ions (Mg^{2+}, Ca^{2+}, Na^+, Cl^-) decreased after purification. Moreover, the K_2O content increased to 54.67% in this experiment. During the purification process, the dissolution temperature, liquid to solid ratio, crystallization temperature and time were very vital for the dissolution and crystallization process. Thus, these four factors were discussed in detail.

3.1.1 Effect of dissolution temperature and liquid to solid ratio. Fig. 1 illustrates the yield for different liquid to solid ratios at temperatures of 100 °C, 80 °C and 60 °C under crystallization temperature of 30 °C and crystallization time of 24 h. Based on Fig. 1, it can be found that the yield increased and reached a plateau with the liquid to solid ratio increasing, and then the yield decreased significantly as the liquid to solid ratio continued to increase at the same temperature. The liquid to solid ratios for the three temperatures (100 °C, 80 °C, 60 °C) were 4 : 1, 4.5 : 1 and 5.3 : 1, respectively. However, the yield (25.35%) was low at 60 °C. Considerably, a high temperature meant high energy consumption and a low temperature represented a low yield. Therefore, the ideal condition was 80 °C with a corresponding 4.5 : 1 liquid–solid ratio.

3.1.2 Effect of crystallization temperature and time. The effect of cooling crystallization temperature and time are illustrated in Fig. 2(a) and (b), respectively. Clearly, crystallization temperature was significant to the yield, which dropped drastically as the temperature increased. However, it was very costly to implement a low temperature in a room environment. Therefore, temperatures such as 20 °C, 25 °C and 30 °C were selected to investigate the relationship between crystallization time and yield. It can be seen from Fig. 2(b) that the crystallization yield initially increased with crystallization time and then reached a plateau until 12 h at each temperature. In addition, the yield was 39.81%, 36.28% and 34.12% at 20 °C, 25 °C and 30 °C, respectively.
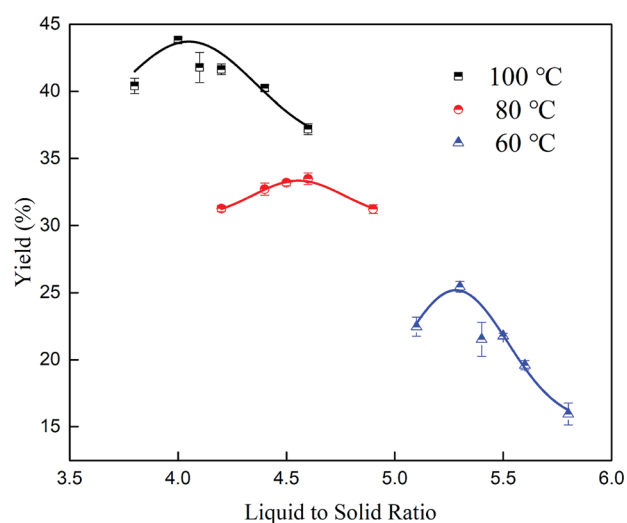

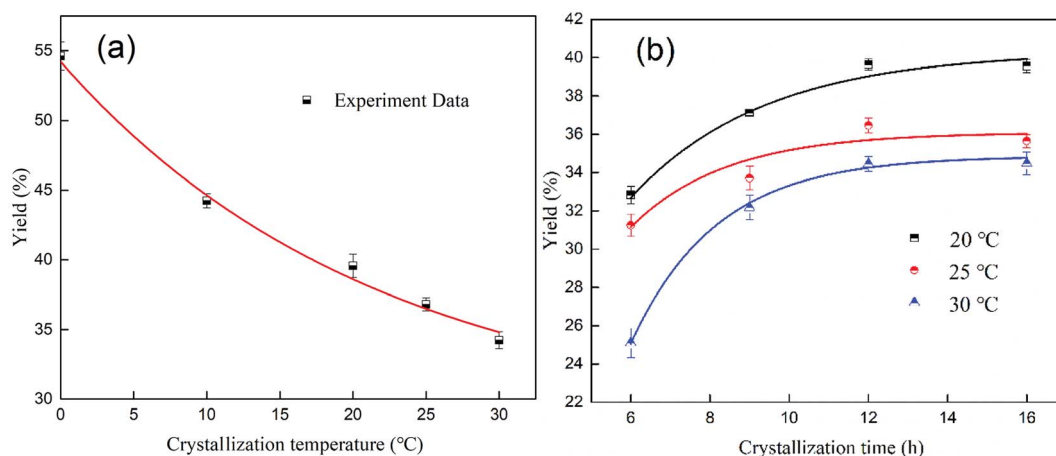**Fig. 1** Effect of the liquid to solid ratio on the yield at different dissolving temperatures.

Fig. 2 Crystallization yield as a function of crystallization temperature (a) and time (b).
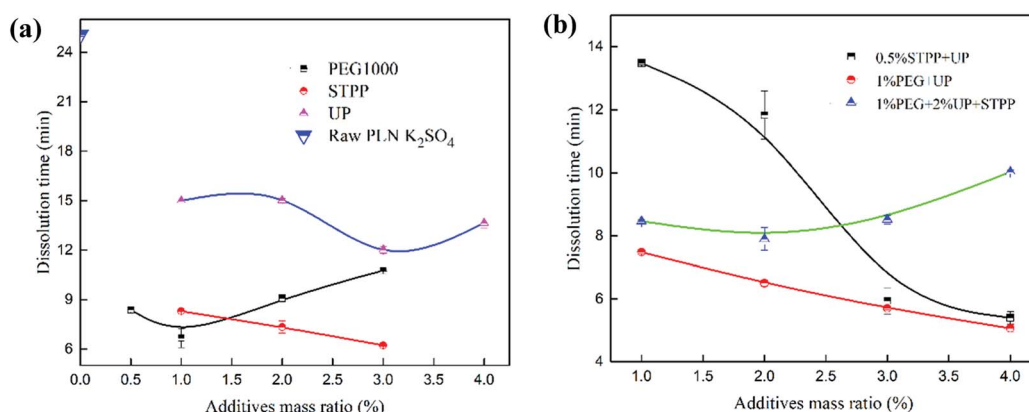

Fig. 3 Effect of a single additive (a) and mix additives (b) on the dissolution time.

3.2 Rapid dissolution of potassium sulfate

After the purification process, the purity of K_2SO_4 significantly improved. The rapid dissolution of K_2SO_4 was investigated in detail. Based on the Noyes–Whitney equation, the diffusion coefficient (D) and diffusion layer thickness (h), which were inherent properties of crystal K_2SO_4, were vital to the dissolution rate.[18,25] Therefore, it is important to improve the D and h by changing K_2SO_4 crystal surface properties. Additives such as the dispersant and wetting agent could change the surface properties of K_2SO_4. These additives could improve the dispersity and wettability, resulting in an intrinsic change in the D and h.[26]

Fig. 3 shows the dissolution time after the K_2SO_4 crystal surface modification with some additives. It can be seen from Fig. 3(a) that addition of additives like PEG, STPP or UP promoted the dissolution of K_2SO_4 and decreased the dissolution time from 25 min to 6.25 min for PLN K_2SO_4. Fig. 3(b) describes the dissolution characteristics for K_2SO_4 with different mass ratios of mixing additives. Only the mass ratio of one additive was changed. Results demonstrated that the dissolution time was shorter by using mixture of additives

rather than using a single additive. In addition, the dissolution time for the 0.5% STPP mass ratio and the 4% UP (0.5% STPP/ 4% UP) with 1% PEG1000/4% UP mass ratio was 5.5 min and 5 min, respectively. When the STPP mass ratio was higher than 0.5% UP, the mixture was difficult to dissolve and the solution became turbid. Moreover, PEG1000 was an expensive organic polymer that was difficult to decompose. In addition, PEG1000 is harmful to the environment and crops. UP and STPP have dispersity and can help to disperse K_2SO_4. Furthermore, UP contains nutrient elements such as N and P, which can promote the growth of plants. Because STPP can be used for softening hard water, it can be applied to hard irrigation water.[27] Moreover, STPP and UP are environment friendly. Therefore, after considering the price and performance of the additives, 0.5% STPP/4% UP was chosen to be the combination additives.

The mechanism for promoting dissolution with additives is depicted in Fig. 4. It is well-known that STPP and UP are dispersants used to prepare suspensions.[28,29] STPP and UP were attached to the surface of K_2SO_4 particles. When the samples were in water, the additives on the surface helped the K_2SO_4 particles to quickly disperse. This phenomenon resulted in an increase in the D and an intrinsic decrease in the h.
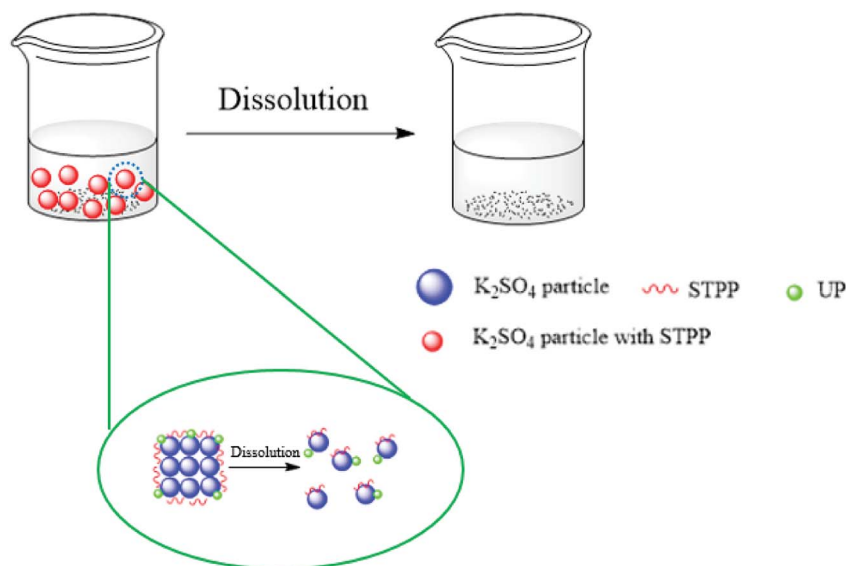
Fig. 4 Mechanism for K_2SO_4 particle dissolution with additives.

Table 5 Effect of crushing time on the particle size distribution

Size fraction (μm)	Crushing time (s)			
	5	10	20	40
+150	26.16	14.30	6.78	2.42
−150 + 74	14.04	12.95	10.78	7.36
−74	59.80	72.75	82.44	90.22
Total	100.00	100.00	100.00	100.00

The particle size was related to the surface area (S).[30–32] The particle size distribution for PLN K_2SO_4 with 0.5% STPP/4% UP varied with crushing time as shown in Table 5. The effect of crushing time on the dissolution time is illustrated in Fig. 5. It can be concluded that the particle size had a significant influence on the dissolution time. As the particle size decreased, the

dissolution time for PLN K_2SO_4 and PLN K_2SO_4 with 0.5% STPP/ 4% UP decreased. In addition, additives containing 0.5% STPP/ 4% UP had an extremely positive effect on the decrease in the dissolution time. As the particle size decreased, the surface area significantly increased, leading to an enhanced S. As a result, the dissolution rate was enhanced.

4 Conclusion

Water soluble potassium sulfate was successfully prepared from LN K_2SO_4 as the raw material. The purity of K_2SO_4 was nearly 100% with a yield of 36.28% after the purification process. Additionally, the rapid dissolution process for K_2SO_4 was realized by the addition of a 0.5% STPP/4% UP additives, which modified the surface properties of the K_2SO_4 particle. This modification resulted in a larger diffusion coefficient (D) and a smaller diffusion layer thickness (h) during the dissolution process. Results also demonstrated that a larger K_2SO_4 surface area (S) improved the dissolution rate.

Conflicts of interest

There are no conflicts of interest to declare.

Nomenclature

dm/dt	Dissolution rate, kg s^{-1}
S	Surface area, m^2
M	Relative molecular mass, g mol^{-1}
h	Diffusion layer thickness, m
D	Diffusion coefficient, m^2 s^{-1}
C	Concentration, mol L^{-1}
m	Mass, kg
t	Time, s
T	Temperature, °C
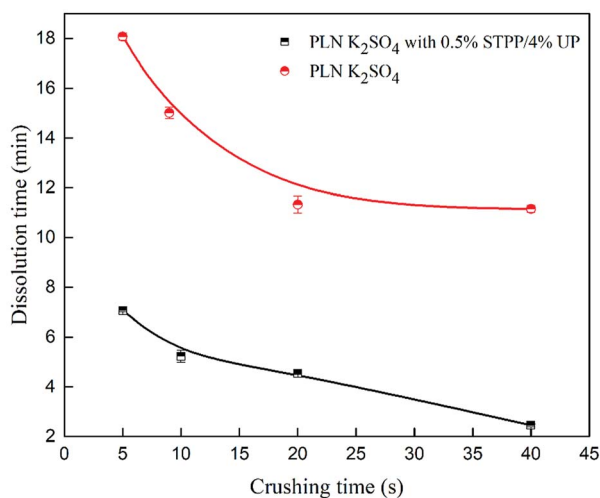
Fig. 5 Effect of particle size on the dissolution time.

Acknowledgements

References

1 I. I. Goncharik, V. V. Shevchuk, N. P. Krut'Ko, A. D. Smychnik and O. A. Kudina, *Russ. J. Appl. Chem.*, 2014, **87**, 1804–1809.

2 K. G. Cassman, T. A. Kerby, B. A. Roberts, D. C. Bryant and S. M. Brouder, *Agron. J.*, 1989, **6**, 870–876.

3 M. Simonsson, S. Andersson, Y. Andrist-Rangel, S. Hillier, L. Mattsson and I. Öborn, *Geoderma*, 2007, **140**, 188–198.

4 J. Niu, W. Zhang, S. Ru, X. Chen, X. Kai, X. Zhang, M. Assaraf, P. Imas, H. Magen and F. Zhang, *Field Crops Res.*, 2013, **140**, 69–76.

5 G. Yaldiz, *Pharmacogn. Mag.*, 2017, **13**, 102–107.

6 S. Su, H. Ma, X. Chuan and B. Cai, *Int. J. Miner. Process.*, 2016, **155**, 130–135.

7 A. V. Litvinovich, O. Y. Pavolva, A. I. Maslova and D. V. Chernov, *Eurasian Soil Sci.*, 2006, **39**, 785–791.

8 K. Kirov, *Bulg. Tyutyun*, 1995, **40**, 13–15.

9 G. I. Rumiantsev, T. M. Khodykina and V. I. Arkhangel'Skiĭ, *Gig. Sanit.*, 1985, **8**, 14–18.

10 S. K. Behera and R. K. Panda, *Agric. Water Manag.*, 2009, **96**, 1532–1540.

11 S. Zhang, V. Sadras, X. Chen and F. Zhang, *Field Crops Res.*, 2013, **151**, 9–18.

12 C. L. Liu, P. C. Jiao, M. L. Wang and Y. Z. Chen, *Miner. Deposits*, 2007, **26**, 322–329.

13 C. L. Liu, M. L. Wang and P. C. Jiao, *Acta Geosci. Sin.*, 2009, **30**, 796–802.

14 M. Zheng, Y. Zhang, X. Liu, Q. I. Wen, F. Kong, N. Zhen and P. U. Linzhong, *Acta Geosci. Sin.*, 2016, **90**, 1195–1235.

15 L. Hao, *Acta Geosci. Sin.*, 2008, **29**, 517–524.

16 Y. Hattori, Y. Haruna and M. Otsuka, *Colloids Surf., B*, 2013, **102**, 227–231.

17 A. A. Noyes and W. R. Whitney, *J. Am. Chem. Soc.*, 2002, **19**, 930–934.

18 A. Anand and G. N. Patey, *J. Phys. Chem. B*, 2018, **122**, 1213–1222.

19 A. Dokoumetzidis, V. Papadopoulou and P. Macheras, *Pharm. Res.*, 2006, **23**, 256–261.

20 A. Xiang and A. J. Mchugh, *J. Membr. Sci.*, 2011, **366**, 104–115.

21 N. Kubota, I. Uchiyama, K. Nakai, K. Shimizu and J. W. Mullin, *Ind. Eng. Chem. Res.*, 1988, **27**, 930–934.

22 N. Kubota, J. Fukazawa, H. Yashiro and J. W. Mullin, *J. Cryst. Growth*, 1995, **149**, 113–119.

23 N. Kubota, Y. Fujisawa, M. Yokota and J. W. Mullin, *J. Cryst. Growth*, 1999, **197**, 388–392.

24 X. Y. Ji, D. L. Chen, T. Wei, X. H. Lu, Y. R. Wang and J. Shi, *Chem. Eng. Sci.*, 2001, **56**, 7017–7024.

25 R. J. Seager, A. J. Acevedo, F. Spill and M. H. Zaman, *Sci. Rep.*, 2018, **8**, 7711.

26 O. A. Slyusar and V. M. Uvarov, *Glass Ceram.*, 2014, **71**, 140–142.

27 C. A. Hodge and T. W. Motes, *Fert. Res.*, 1994, **39**, 59–69.

28 H. Tan, Y. Guo, B. Ma, J. Huang, B. Gu and F. Zou, *KSCE J. Civ. Eng.*, 2018, **22**, 2934–2941.

29 H. Tan, F. Zou, B. Ma, M. Liu, X. Li and S. Jian, *Constr. Build. Mater.*, 2016, **126**, 617–623.

30 S. Wu, B. Yu, Z. Wu, S. Fang, B. Shi and J. Yang, *RSC Adv.*, 2018, **8**, 8544–8551.

31 J. Yu, L. Sun, C. Berrueco, B. Fidalgo, N. Paterson and M. Millan, *J. Anal. Appl. Pyrolysis*, 2018, **130**, 127–134.

32 M. Liu, M. Shabaninejad and P. Mostaghimi, *J. Pet. Sci. Eng.*, 2018, **170**, 130–138.